

<b>REPORT DOCUMENTATION PAGE</b>			<i>Form Approved</i> <i>OMB No. 0704-0188</i>	
Public reporting burden for this collection of information is estimated to average 1 hour per response, including the time for reviewing instructions, searching existing data sources, gathering and maintaining the data needed, and completing and reviewing this collection of information. Send comments regarding this burden estimate or any other aspect of this collection of information, including suggestions for reducing this burden to Department of Defense, Washington Headquarters Services, Directorate for Information Operations and Reports (0704-0188), 1215 Jefferson Davis Highway, Suite 1204, Arlington, VA 22202-4302. Respondents should be aware that notwithstanding any other provision of law, no person shall be subject to any penalty for failing to comply with a collection of information if it does not display a currently valid OMB control number. <b>PLEASE DO NOT RETURN YOUR FORM TO THE ABOVE ADDRESS.</b>				
<b>1. REPORT DATE (DD-MM-YYYY)</b> 31/08/2015		<b>2. REPORT TYPE</b> Final Technical Report		<b>3. DATES COVERED (From - To)</b> 01/09/2014 - 31/08/2015
<b>4. TITLE AND SUBTITLE</b>  Development of Fast Deterministic Physically Accurate Solvers for Kinetic Collision Integral for Applications of Near Space Flight and Control Devices Final Technical Report			<b>5a. CONTRACT NUMBER</b> GS04T09DBC0017	
			<b>5b. GRANT NUMBER</b>	
			<b>5c. PROGRAM ELEMENT NUMBER</b>	
<b>6. AUTHOR(S)</b>  Alekseenko, Alexander			<b>5d. PROJECT NUMBER</b> PP-SAS-KY06-001-P3	
			<b>5e. TASK NUMBER</b>	
			<b>5f. WORK UNIT NUMBER</b>	
<b>7. PERFORMING ORGANIZATION NAME(S) AND ADDRESS(ES)</b> High Performance Technologies Innovations LLC 4803 Stonecroft Blvd. Chantilly, VA 20151			<b>8. PERFORMING ORGANIZATION REPORT NUMBER</b>  PP-SAS-KY06-001-P3-D6	
<b>9. SPONSORING / MONITORING AGENCY NAME(S) AND ADDRESS(ES)</b> Department of Defense High Performance Computing Modernization Program Office 10501 Furnace Road Suite 101 Lorton, VA 22079			<b>10. SPONSOR/MONITOR'S ACRONYM(S)</b> HPCMP, PETTT	
			<b>11. SPONSOR/MONITOR'S REPORT NUMBER(S)</b>	
<b>12. DISTRIBUTION / AVAILABILITY STATEMENT</b>  DISTRIBUTION A. Approved for public release: distribution unlimited; Case #: 88ABW-2016-0252				
<b>13. SUPPLEMENTARY NOTES</b>				
<b>14. ABSTRACT</b>  This document is the Final Technical Report for the PETTT Pre-planned Project, PP-SAS-KY06-001-P3, Development of Fast Deterministic Physically Accurate Solvers for Kinetic Collision Integral for Applications of Near Space Flight and Control Devices. The development of predictive capabilities for modeling spacecraft environments in the near-space regime for re-entry applications and for satellite trajectories presents significant challenges due to the multi-physics, multi-scale nature of the flows of interest. A challenge directly related to the multi-scale flows over space vehicles is accurate numerical prediction of flows that contain most or all gas dynamic regimes from continuum to rarefied to free molecular. To address this problem, the goal of this project is the improvement of gas dynamics solvers that are currently used across several DoD applications. Significant steps were taken toward the goal by achieving the following objectives; The implementation of a new BGK-type model with velocity-dependent collision frequency and an increased fidelity in relaxation of momenta; The development of methods for fast evaluation of the Boltzmann collision integral based on the stochastic integration; and The validation of the improved physical accuracy of the new modules.				
<b>15. SUBJECT TERMS</b> PETTT, HPC, HPCMP, supersonic and hypersonic flows; space systems; re-entry and high altitude flows; deterministic solution of the Boltzmann equation; nodal discontinuous Galerkin discretizations; non-continuum gas flows; shock wave flows; SMOKE solver; <span style="float: right;">+</span>				
<b>16. SECURITY CLASSIFICATION OF:</b> Unclassified			<b>17. LIMITATION OF ABSTRACT</b>  UU	<b>18. NUMBER OF PAGES</b>  24
<b>a. REPORT</b> Unclassified	<b>b. ABSTRACT</b> Unclassified	<b>c. THIS PAGE</b> Unclassified		
				<b>19b. TELEPHONE NUMBER (include area code)</b> 703-812-8205



**Development of Fast Deterministic Physically Accurate Solvers for Kinetic Collision Integral for Applications of Near Space Flight and Control Devices**

**PP-SAS-KY06-001-P3  
Deliverable D6**

**Final Technical Report**

Submitted by  
*Alexander Alekseenko (California State University Northridge)*  
31 August 2015

for  
User Productivity Enhancement, Technology Transfer, and Training  
(PETTT) Program

High Performance Computing Modernization Program (HPCMP)



Contract No.: GS04T09DBC0017

**Government Users/Sponsors/Partners: Dr. Eswar Josyula (AFRL/RQHF)**

## TABLE OF CONTENTS

<b>1. OVERVIEW .....</b>	<b>1</b>
1.1 Summary of the Accomplishments.....	1
1.1.1 <i>Objective 1. The implementation of a new BGK-type model with velocity-dependent collision frequency and an increased fidelity in relaxation of moments. ...</i>	<i>1</i>
1.1.2 <i>Objective 2. The development of methods for fast evaluation of the Boltzmann collision integral based on the stochastic integration. ....</i>	<i>2</i>
1.1.3 <i>Objective 3. Validation of the improved physical accuracy of the new modules.....</i>	<i>2</i>
1.2 Areas of Applicability of the Proposed Software .....	2
1.3 Potential Impact of the Project .....	2
<b>2. ACCOMPLISHMENTS.....</b>	<b>3</b>
2.1 Key Components of DGVlib .....	4
2.2 DGVlib Components and Functionality.....	4
2.2.1 <i>Subroutines Implementing Nodal Discontinuous Galerkin Discretizations in the Velocity Variable.....</i>	<i>4</i>
2.2.2 <i>Subroutines Implementing Collision Operators in Gas-Kinetic Equations.....</i>	<i>4</i>
2.2.3 <i>The Use of DGVlib with 0D, 1D, and 2D Solvers.....</i>	<i>5</i>
2.3 Mathematical Models Utilized in DGVlib.....	6
2.3.1 <i>Dimensionless Reduction of the Velocity Variable .....</i>	<i>6</i>
2.3.2 <i>BGK Model with Velocity-Dependent Collision Frequency .....</i>	<i>7</i>
2.3.3 <i>BGK-Type Model with Exact Enforcement of Moments .....</i>	<i>7</i>
2.3.4 <i>Extended Model for Enforcing Relaxation Rates .....</i>	<i>8</i>
2.3.5 <i>Implementation of Korobov Integration for Evaluating the Collision Operator.....</i>	<i>10</i>
2.4 Numerical Accuracy and Validation.....	12
2.4.1 <i>Simulations in Zero Spatial Dimensions Using the Improved Velocity-Dependent Collision Frequency .....</i>	<i>12</i>
2.4.2 <i>Efficiency of the Evaluation of Boltzmann Collision Integral using Korobov Nodes</i>	<i>14</i>
2.4.3 <i>Simulation of One Dimensional Supersonic Flow: the Normal Shock Wave</i>	<i>14</i>
2.4.4 <i>Simulation of Two-Dimensional Supersonic Flow around a Cylinder.....</i>	<i>16</i>

**3. SUMMARY ..... 20**  
**4. REFERENCES..... 21**

## 1. OVERVIEW

This Final Technical Report constitutes the completion of the PETTT Pre-Planned Project PP-SAS-KY06-001-P3.

The development of predictive capabilities for modeling spacecraft environments in the near-space regime for re-entry applications and for satellite trajectories presents significant challenges due to the multi-physics, multi-scale nature of the flows of interest. A challenge directly related to the multi-scale flows over space vehicles is accurate numerical prediction of flows that contain most or all gas dynamic regimes from continuum to rarefied to free molecular. To address this problem, the goal of this project is the improvement of gas dynamics solvers that are currently used across several DoD applications. Significant steps were taken toward the goal by achieving the following objectives

- (1) The implementation of a new BGK-type model with velocity-dependent collision frequency and an increased fidelity in relaxation of moments,
- (2) The development of methods for fast evaluation of the Boltzmann collision integral based on the stochastic integration,
- (3) The validation of the improved physical accuracy of the new modules.

### 1.1 Summary of the Accomplishments

#### 1.1.1 *Objective 1. The implementation of a new BGK-type model with velocity-dependent collision frequency and an increased fidelity in relaxation of moments.*

The following major tasks were completed to achieve the first objective of the proposal.

- (1) A stand-alone library, DGVlib, was developed to encompass the following software tools:
  - a. Subroutines for nodal discontinuous Galerkin (DG) discretizations of the kinetic equations in the velocity variables on uniform and octree meshes;
  - b. Subroutines for evaluating the collision operator using BGK-type model with velocity dependent collision frequency;
  - c. Subroutines for evaluating Boltzmann collision operator using nodal DG discretizations on uniform grids and subroutines to pre-compute values of the collision kernel.
- (2) The BGK model with velocity dependent collision frequency was generalized to allow for a large number of moments to be enforced approximately. Subroutines implementing the extended model were added to the library.
- (3) Techniques for automatic selection of the kinetic collision model were developed and implemented in the library. The evaluation of the kinetic collision operator can be accomplished by a call of a single subroutine which will choose an appropriate kinetic model based on the norm of deviation of the solution from the continuum state.
- (4) The DGVlib library has been merged with a number of drivers implemented in Fortran. Specifically, it was merged with a high order multi-step time integration driver in zero spatial dimensions and with a high order Runge-Kutta DG driver in one spatial dimension that were available to the PI. The library was merged with a second order

accurate finite volume two dimensional solver SMOKE available to the co-PI Gimelshein. The software that resulted from the merger was used to perform validation of the library accuracy described in Objective 3. The library was also merged with a C++ driver, the Unified Flow Solver.

(5) A detailed user guide was developed to help the user utilize DGVlib.

### ***1.1.2 Objective 2. The development of methods for fast evaluation of the Boltzmann collision integral based on the stochastic integration.***

For the second objective, a new numerical method was designed for evaluating nodal-DG discretizations of the Boltzmann collision operator on uniform grids based on Korobov integration. The method requires pre-computing and storing values of the kernel of the collision operator at quasi-stochastic nodes. Subroutines for computing and storing values of the kernel and subroutines for evaluating the collision integral using quasi-stochastic Korobov quadratures were developed and added to the library. Accuracy tests of the new method were performed.

### ***1.1.3 Objective 3. Validation of the improved physical accuracy of the new modules.***

Solutions to the following problems were computed using the new models of DGVlib library.

- (1) Problems of spatially homogeneous relaxation were solved to study in detail the properties of the new models of collision integral.
- (2) One dimensional problems of normal shock wave were solved for Mach numbers 1.55, 3.00, 3.8, 6.5, and 9.0.
- (3) Two dimensional super-sonic flow past cylinder was computed.

Zero-dimensional solutions were compared to solutions to the full Boltzmann equation. One and two dimensional solutions were compared to DSMC solutions computed by an established code SMILE. **Solutions computed by new models showed a significant improvement in predicting temperature profiles of the flows and improvement in predicting density profiles of the flows as compared to the classical ES-BGK model.**

## **1.2 Areas of Applicability of the Proposed Software**

The developed software capability is expected to provide essential elements for the integration and generalization of kinetic and hybrid solvers, both currently used and to be developed in DoD. It primarily targets various AF applications where flow non-equilibrium is important, such as hypersonic flight at moderate to high altitudes and rocket propulsion with plume - atmosphere interaction, both for conventional and miniaturized thrusters, as well as transient rarefied flows. DGVlib, made available to DoD researchers and engineers, will allow for expanding the area of applicability of the existing fluid dynamics codes, and stimulate the development of state-of-the-art hybrid codes applicable to all flow regimes from continuum to free molecular.

## **1.3 Potential Impact of the Project**

The Air Force is focused on the development of advanced space technologies for more effective, more affordable warfighter missions. To make progress in this area, it is necessary to develop predictive capabilities for modeling spacecraft environments in the near-space regime for reentry

applications as well as for satellite trajectories. Other DoD programs that rely critically on technologies in this flight regime are AF's global strike weapons and boost glide vehicles, as well as MDA's exoatmospheric anti-ballistic missiles programs. The availability of efficient and physically accurate predictive tools for gas flow modeling in a wide range of flow regimes is critical for the evaluation of local and overall aerothermodynamic loads and the detailed analysis of existing and future propulsion systems. Computer model based tools are also one of the central components of the space situational awareness, where the comprehensive knowledge of space objects and the ability to track, understand and predict their future location becomes the key.

The developed software library addressed several improvements in the existing solvers.

- The implemented BGK model collision operator with velocity dependent collision frequency was shown to increase physical accuracy in predicting temperature profiles of non-continuum flows. With the availability of this module a user gains additional flexibility on what properties of the solution may be enforced in the kinetic models at moderate additional computational costs.
- The implemented module performing integration of the collision integral using Korobov nets computes the Boltzmann collision operator faster than full deterministic integral evaluation.
- The modules that implement fully deterministic solution of the Boltzmann equation can be conveniently used to provide accurate solutions, although these solutions will not be efficient.
- The implemented algorithms for choosing a different kinetic model based on the norm of deviation of the solution from continuum provide a convenient tool to use in kinetic simulations when the most efficient model can be used to compute the collision operator at a point.

Overall, the implemented software has high potential to improve gas dynamics solvers that are currently used across several DOD platforms. Through that, the implemented software has potential to address the following problems pertaining to the Space and Astrophysical Sciences area: (1) modeling of near-space vehicle aerothermodynamics for flight conditions where there are both continuum and rarefied flow regions, (2) spacecraft thrusters that exhaust high density plumes into rarefied atmosphere, (3) gas flows in microscale onboard devices. The completed project benefits the following DOD research topics: MDA12-022 “Miniature extendable nozzles or actuating nozzles for improved ISP of DACS thrusters”; AF141-089 “Electric propulsion of orbit transfer”, and MDA12-009 “Fast-running physics-based models for intercept debris aero-heating and aero-thermal demise”.

## **2. ACCOMPLISHMENTS**

A software library, DGVlib, has been developed to encompass a set of tools that can be used to solve kinetic equations of gas dynamics. The name of the library, DGVlib, stands for nodal-Discontinuous Galerkin discretizations in the Velocity variable (nDGV). The library includes subroutines to perform nDGV discretizations in the three dimensional velocity space including capabilities for non-uniform octree discretizations, subroutines for evaluating collision operators in gas-kinetic models, including the BGK, ES-BGK and the new velocity-dependent BGK model

with velocity dependent collision frequency. The library includes subroutines to evaluate the Boltzmann collision integral using Korobov quadratures. DGVlib library was merged with a high order multiple time stepping driver in zero spatially dimensions, a high order Runge-Kutta discontinuous Galerkin driver in one spatial dimension, and with the second order accurate finite volume solver SMOKE in two spatial dimensions. The resulting codes were used to perform benchmark simulations which include problems of spatially homogeneous relaxation, normal shock wave and super-sonic flow past cylinder.

## 2.1 Key Components of DGVlib

The new software library has the following key components:

1. A collection of subroutines to build elements, nodes, and basis functions of nodal discontinuous Galerkin discretizations of functions in three dimensional velocity space.
2. Subroutines for evaluation of the collision operators in gas kinetic models, including the BGK, the ES-BGK, and the new velocity-dependent BGK model with velocity dependent collision frequency.
3. Subroutines for the evaluation of the Boltzmann collision operator using Korobov quadratures.
4. Interfaces to call collision operator subroutines from other solvers in zero, one and two spatial dimensions.

## 2.2 DGVlib Components and Functionality.

The overall structure of the DGVlib is shown in Figure 1. Key capabilities and main features of the library are described below.

### 2.2.1 *Subroutines Implementing Nodal Discontinuous Galerkin Discretizations in the Velocity Variable.*

DGVlib includes subroutines to create rectangular meshes in 3D velocity space. It also includes subroutines to create octree non-uniform meshes in 3D velocity space; however, octree meshes are not supported by the subroutines evaluating the collision operators. At the core of the library are subroutines implementing high order nodal discontinuous Galerkin discretization in the velocity space (nDGV) [1]. Subroutines for interpolating nDGV solutions from the Galerkin coefficients are also included. The library maintains two nDGV discretizations, referred as the primary and the secondary meshes in Figure 1. nDGV discretizations are functionally very similar to, albeit more powerful than, discrete ordinate discretizations of kinetic equations which are commonly used for simulations of rarefied gas dynamics. As a result, DGVlib can be merged relatively easily with kinetic solvers that are based on the discrete ordinate approach. A folder view of DGVlib merged with a zero dimensional solver is shown in Figure 2.

### 2.2.2 *Subroutines Implementing Collision Operators in Gas-Kinetic Equations.*

DGVlib includes several subroutines that implement evaluation of the collision operators in gas kinetic equations. The following models are supported: the BGK model, the ES-BGK model, and the new BGK model with the velocity dependent collision frequency [2]. In addition, the library

implements evaluation of the full Boltzmann collision operator using the formulation of [1] directly and using Korobov quadratures. The BGK model with velocity-dependent collision frequency relies on evaluation of the full collision operator to determine the correct relaxation rates in the solution. All models are supported on the primary mesh. Also, deterministic evaluation of the full collision operator is supported on the secondary mesh. Model collision operators are not yet supported on the secondary mesh, since there has been no user demand for this feature. A conglomerate subroutine is provided for the evaluation of the collision operator on the primary mesh, called `UniversalCollisionOperatorDGV` that automatically chooses the model based on the degree of deviation of the solution from the local Maxwellian distribution.

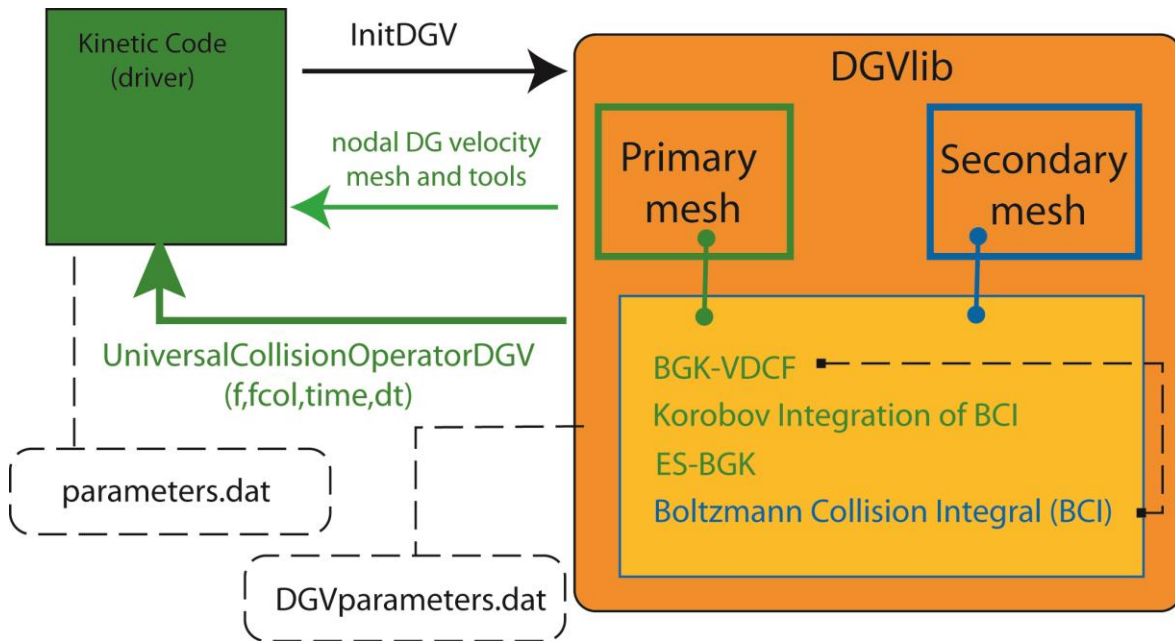


Figure 1. Functionality of DGVlib within a kinetic solver.

### 2.2.3 The Use of DGVlib with 0D, 1D, and 2D Solvers.

The library is to be called from an external driver. First, DGVlib subroutines for creating nDGV discretizations are called to construct the discretization in the velocity variable. Then, the arrays that implement the velocity discretization are passed to the driver to construct the full spatial and velocity discretization. In the case of 1D and 2D applications, discretizations in the spatial variables are provided by the driver. Currently, the complete spatial and velocity discretization is obtained by taking the full tensor product. As a result, all spatial cells have the same velocity discretization. To invoke kinetic collision operators in 1D and 2D applications, subroutines are provided that evaluate the collision operator over a collection of spatial cells referenced by a single index. The library maintains data structures to store auxiliary information about the solution at each spatial cell. In particular, the library stores relaxation rates computed for each spatial cell that are used in the BGK model with velocity dependent collision frequency. It also keeps track of when the rates have to be updated.

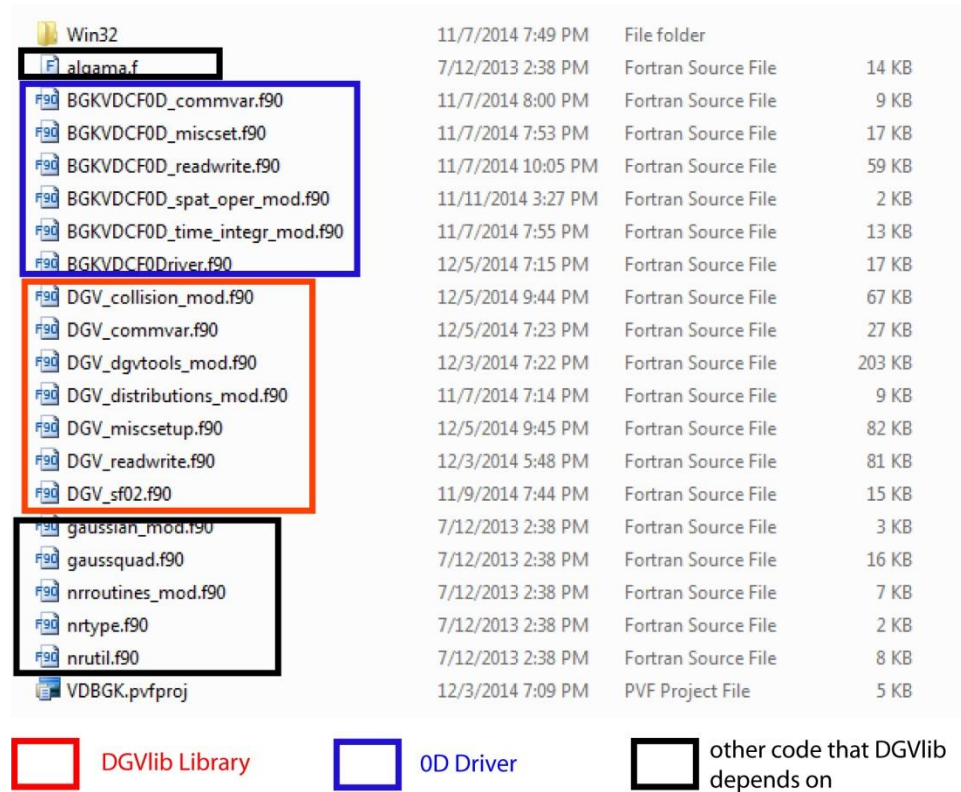


Figure 2. A folder view of DGVlib library merged with a zero dimensional driver.

## 2.3 Mathematical Models Utilized in DGVlib

DGVlib library encompasses subroutines implementing the recently proposed BGK-type (Bhatnagar-Gross-Krook) model with velocity-dependent collision frequency and increased fidelity in relaxation of moments and subroutines that implement integration of the Boltzmann collision integral using Korobov nodes. In addition, subroutines for evaluating the classical BGK model and the ellipsoidal-statistical BGK model and subroutines for evaluating the full Boltzmann collision operator using the formulation of [1] are also included in the library. The following sections briefly summarize the mathematical models that are employed in the first two approaches. Additional discussion and also detail on the other implemented models can be found in Appendix A to this report.

### 2.3.1 Dimensionless Reduction of the Velocity Variable

Gas dynamic constants vary greatly in scale. Caution should be exercised when these quantities are combined in a numerical method in order to avoid accumulation of the round-off errors. However, because of the large number of integration points, accumulation of round-off errors is difficult to avoid in evaluation of the collision operator. The use of dimensionless reduction when all the key quantities are of the order of unit can help avoid many obstacles caused by the round-off errors. DGVlib uses the dimensionless reduction that can be found in Chapter 3 in [3]. Below, the key relations are very briefly summarized.

Let  $\hat{t}$ ,  $\hat{x}$ ,  $\hat{v}$  be the conventional dimensional variables of time, space and velocity. Their dimensionless counterparts are defined by

$$t = \frac{\hat{t}}{\mathbb{T}}, \quad x_i = \frac{\hat{x}}{L}, \quad v = \frac{\hat{v}}{C_\infty}, \quad \text{or} \quad \hat{t} = t\mathbb{T}, \quad \hat{x} = xL, \quad \hat{v} = vC_\infty,$$

Where  $T_\infty$  is some reference temperature and  $L$  is some reference length scale. The reference velocity  $C_\infty$  is conventionally defined by  $C_\infty = \sqrt{2RT_\infty}$  where  $R$  is the gas constant. The reference time scale  $\mathbb{T}$  is defined by  $\mathbb{T} = L/C_\infty$ .

The dimensionless density, bulk velocity and temperature are defined by

$$n(t, x) := \int_{R^3} f(t, x, v) dv \quad n(t, x)\bar{u}(t, x) := \int_{R^3} v f(t, x, v) dv$$

$$n(t, x)T(t, x) := \frac{2}{3} \int_{R^3} (v - \bar{u})^2 f(t, x, v) dv$$

Here the dimensionless velocity distribution function  $f(t, x, v)$  is given by

$$f(t, x, v) = \frac{L^3 C_\infty^3}{N} \hat{f}(\hat{t}, \hat{x}, \hat{v}),$$

where  $N$  is the total number of molecules in the volume of gas  $L^3$ . Mathematical models presented in this section are given in the dimensionless variables.

### 2.3.2 BGK Model with Velocity-Dependent Collision Frequency

This section briefly describes the BGK-type models with the velocity dependent collision frequency that are implemented in the subroutine EvalColVelES. Two models are used in this approach. The first model will attempt to enforce exactly the relaxation rates for the selected group of moments. In this approach the number of enforced moments and the number of basis functions in the representation of the collision frequency have to be the same. A linear system of equations is solved at every time step to determine the coefficients in the representation of the collision frequency. In the second model, the number of enforced moments is greater than the number of basis functions. A linear least squares problem is solved at every time step to determine the coefficients of the collision frequency. The two models are summarized below.

### 2.3.3 BGK-Type Model with Exact Enforcement of Moments

Let  $\psi_i(\vec{u})$ ,  $i = 0, \dots, k$  be a collection of linearly independent functions in velocity space. To allow the BGK model freedom to accommodate the specified relaxation frequencies for selected solution moments one assumes that the collision frequency has the form

$$\nu(t, \vec{u}) = \sum_{i=0}^k c_i(t) \psi_i(\vec{u}).$$

In general, it is best to select functions  $\psi_i(\vec{u})$  so that the projection mapping between the kernels of the enforced moments and the functions  $\psi_i(\vec{u})$  is invertible and is well-conditioned in a weighted  $L^2$ -norm with  $f_M(t, \vec{u})$  serving as the weight. In simulations presented in the Section 3 the following functions  $\psi_i(\vec{u})$  were used:

$$\begin{aligned} \psi_0(\vec{u}) &= 1, \quad \psi_1(\vec{u}) = u_1, \quad \psi_2(\vec{u}) = u_2, \quad \psi_3(\vec{u}) = u_3, \quad \psi_4(\vec{u}) = u_1^2 + u_2^2 + u_3^2, \\ \psi_i(\vec{u}) &= P_{i-3}(u_1), \quad i = 5, \dots, 8, \end{aligned}$$

where  $P_l(u_1)$  are the Legendre polynomials of degree  $l$ . It is assumed that the coefficient standing with  $\psi_0(\vec{u})$  has the form  $c_0 + \nu_{\text{BGK}}$ . Thus one seeks an addition to the collision frequency of the classical BGK model that enforces relaxation speeds of selected moments. With this assumption, the new model may be considered as a generalization of the classical BGK model.

The coefficients  $c_i(t)$ ,  $i = 1, \dots, k$  are determined from the condition that moments  $f_\varphi(t)$  of the solution relax with the prescribed relaxation frequencies  $\nu_\varphi$ . Specifically, the following system is solved at each time step:

$$(\nu_\varphi(t) - \nu_{\text{BGK}})(f_\varphi^M - f_\varphi) = \sum_{i=0}^k c_i(t) \int_{R^3} \psi_i(\vec{u})(f_M(t, \vec{u}) - f(t, \vec{u}))\varphi(\vec{u}) du.$$

The relaxation frequencies are determined by evaluating the full Boltzmann collision integral using the formula:

$$\nu_\varphi(t) = -\frac{\hat{I}_\varphi}{f_\varphi(t) - f_\varphi^M(t)}$$

Where  $\hat{I}_\varphi$  is the Galerkin projection of the Boltzmann collision operator up to coefficients arising in dimensionless reduction. The kernels  $\varphi(\vec{v})$  run over the set  $\varphi_1(\vec{v}), \dots, \varphi_k(\vec{v})$  that determine which properties are enforced in the solution.

### 2.3.4 Extended Model for Enforcing Relaxation Rates

The model with exact enforcement of moments has one undesired property, namely that the kinetic models can become stiff (more stiff than the classical models) if relaxation rates are enforced for higher order moments. To reduce the stiffness one can change the way in which the relaxation rates of moments are enforced.

**DISTRIBUTION A.** Approved for public release: distribution unlimited.

In the model of the previous section, the number of functions  $\psi_k(\vec{v})$  and the number of enforced moments  $f_\varphi(t)$  is the same, resulting in a linear system of equations with a square matrix. In principle, one may desire to enforce relaxation rates for a larger number of moments than the number of function  $\psi_i(\vec{v})$ . In this case, the linear system of the previous section is overdetermined, that is, has a rectangular matrix.

It will be assumed that the collision frequency  $\nu$  is expressed in terms of basis functions  $\psi_k(\vec{v})$  and corresponding coefficients  $c_k(t, \vec{x})$ ,  $k = 1 \dots N_b$ , as

$$\nu(t, \vec{x}, \vec{v}) = \sum_{k=1}^{N_b} c_k(t) \psi_k(\vec{v}).$$

For convenience of later use, a vector of parameters,  $\vec{c}$ , is defined as

$$\vec{c} \equiv (c_1, c_2, \dots, c_{N_b})^T.$$

For any function  $\phi(\vec{v})$ , the corresponding (generalized) moment can be defined as

$$f_\phi(t, \vec{x}) \equiv \int_{R^3} \phi(\vec{v}) f(t, \vec{x}, \vec{v}) dv.$$

Further, given any selection of moments  $\phi_i(\vec{v})$  for  $i = 1 \dots N_c$ , one can obtain the rate of evolution (due to collisions) of any moment based on a weak form of the Boltzmann equation as,

$$\dot{M}_{\phi_i}^e \equiv \partial_t f_{\phi_i} |_{\text{collision}} = I_{\phi_i},$$

where the right hand side of the above equation can be conveniently evaluated using certain symmetry properties of the collision operator. These properties ensure that the above right hand side term is zero for collision invariants.

Similarly, the rate of evolution obtained from the model approximations of the collision operator can be expressed as,

$$\dot{M}_{\phi_i}^a \equiv \int_{R^3} \phi_i(\vec{v}) \nu(t, \vec{x}, \vec{v}) (f_0(t, \vec{x}, \vec{v}) - f_0(t, \vec{x}, \vec{v})) dv.$$

Based on the assumed functional form of  $\nu$ , in terms of basis functions  $\psi_k(\vec{v})$ , the rate of evolution of the generalized moment can be expanded as,

$$\begin{aligned} \dot{M}_{\phi_i}^a(\vec{c}) &= \int \phi_i(\vec{v}) \left( \sum_{k=1}^{N_b} c_k \psi_k(\vec{v}) \right) (f_0(t, \vec{x}, \vec{v}) - f_0(t, \vec{x}, \vec{v})) dv \\ &= \sum_{k=1}^{N_b} G_{ik} c_k = [\vec{G}] [\vec{c}], \end{aligned}$$

where

$$G_{ik} = \int \phi_i(\vec{v}) \psi_k(\vec{v}) (f_0(t, \vec{x}, \vec{v}) - f_0(t, \vec{x}, \vec{v})) dv.$$

In order to determine the unknown coefficients  $c_k(t, \vec{x})$ , one defines an error measure  $e$  and seeks those coefficients that minimize the error. The error function  $e$  is chosen to be in the following form:

$$e = \sum_{i=1}^{N_c} \left[ \dot{M}_{\phi_i}^e - \dot{M}_{\phi_i}^a(\vec{c}) \right]^2 = \sum_{i=1}^{N_c} \left[ \dot{M}_{\phi_i}^e - [G] [\vec{c}] \right]^2,$$

where  $N_c$  denotes the number of constraints on evolution of moments that we choose to consider. One can see that the minimization of  $e$  is a classical linear least squares problem to which standard approaches can be applied. In particular, if the matrix  $G$  is full rank then the solution to the problem is given by

$$\vec{c} = [G^T G]^{-1} G^T \dot{M}_{\phi_i}^e.$$

If a matrix  $G$  is ill-conditioned or even not full rank, the problem can be regularized using the singular value decomposition.

### 2.3.5 Implementation of Korobov Integration for Evaluating the Collision Operator

Stochastic evaluation of the Boltzmann collision integral has been the most successful approach for obtaining solutions in multidimensional applications [4]. Stochastic methods are, indeed, the only well-developed methods that beat the "curse of dimensionality" in multidimensional integration. A family of efficient quadratures is due to Korobov [5], who proposed the use of decimal parts of fractions as Monte-Carlo integration points and showed that the resulting quasi-stochastic multidimensional quadratures converge fast in the case of smooth periodic functions. A description of the Korobov quadratures implemented in DGVlib can be found in Chapter 3 Section 24 of [5]. This section briefly summarizes the algorithm implemented in DGVlib.

Let a multidimensional function  $h(x_1, \dots, x_s)$  be periodic with period one on a  $s$ -dimensional cube  $D = ([0, 1])^s$ . Let  $h(x_1, \dots, x_s)$  have an absolutely converging Fourier series on  $D$  with Fourier coefficients  $C(m_1, \dots, m_s)$  satisfying the inequality

**DISTRIBUTION A.** Approved for public release: distribution unlimited.

$$C(m_1, \dots, m_s) \leq \frac{C}{(\bar{m}_1 \dots \bar{m}_s)^\alpha}, \quad \text{where } \bar{m} = \max(1, |m|), \text{ for some } \alpha > 1.$$

Consider the quadrature formula

$$\int_0^1 \dots \int_0^1 h(x_1, \dots, x_s) dx_1 \dots dx_s = \frac{1}{p} \sum_{k=1}^p h\left(\left\{\frac{a_1 k}{p}\right\}, \dots, \left\{\frac{a_s k}{p}\right\}\right) - R_p[h],$$

where  $p$  is a large number,  $a_i$ ,  $i = 1, \dots, s$ , are some whole numbers relatively prime with  $p$ , and  $\{\cdot\}$  stands for the fractional (decimal) part of the number. The following estimate holds for the truncation error:

$$|R_p[h]| \leq C_1(\alpha, s) \frac{\ln^{\alpha s} p}{p^\alpha}.$$

It follows that the convergence rate  $\alpha$  is proportional to the smoothness of the function. Specifically, a higher smoothness of the function  $h$  implies the faster convergence rate of the quadrature rule.

Subroutines of DGVlib implement the Korobov integration of the Galerkin projection of the Boltzmann collision integral (see Appendix A and also [1])

$$\begin{aligned} \hat{I}_{\hat{\phi}_p^j} &= \frac{N^2 \hat{d}^2 C_\infty}{L^6} \int_{R^3} \int_{R^3} f(t, \vec{x}, \vec{v}) f(t, \vec{x}, \vec{u}) A(\vec{v}, \vec{u}; \phi_p^j) du dv \\ &\approx \frac{N^2 \hat{d}^2 C_\infty}{L^6} \sum_{k=1}^p \sum_{k=1}^p f(t, \vec{x}, \vec{v}_k) f(t, \vec{x}, \vec{u}_k) \tilde{A}(\vec{v}_k, \vec{u}_k; \phi_p^j), \end{aligned}$$

where

$$\tilde{A}(\vec{v}_k, \vec{u}_k; \phi_p^j) = \frac{(\Delta V)^2}{p} A(\vec{v}_k, \vec{u}_k; \phi_p^j)$$

and  $V = [u_L, u_R] \times [v_L, v_R] \times [w_L, w_R]$  is the velocity domain, and  $\Delta V$  is the volume of the domain  $V$ . The Korobov nodes  $\vec{v}_k$ ,  $\vec{u}_k$  are obtained by scaling, i.e.,

$$\begin{aligned} \vec{v}_k &= \left( \frac{a_1 k}{p} (u_R - u_L) + u_L, \frac{a_2 k}{p} (v_R - v_L) + v_L, \frac{a_3 k}{p} (w_R - w_L) + w_L \right) \\ \vec{u}_k &= \left( \frac{a_4 k}{p} (u_R - u_L) + u_L, \frac{a_5 k}{p} (v_R - v_L) + v_L, \frac{a_6 k}{p} (w_R - w_L) + w_L \right) \end{aligned}$$

The summation kernel  $\tilde{A}(\vec{v}_k, \vec{u}_k; \phi_p^j)$  is pre-computed and stored for future use.

## 2.4 Numerical Accuracy and Validation

### 2.4.1 Simulations in Zero Spatial Dimensions Using the Improved Velocity-Dependent Collision Frequency

The PIs developed an improved model for enforcing relaxation rates using a velocity-dependent collision frequency. The mathematical approach to the new velocity-dependent collision frequency is described in [2,6]. The new approach has been implemented in the DGVlib library. This section summarizes the advantages of the new model in the solution to the problem of spatially homogeneous relaxation of two Maxwellian streams.

The two Maxwellian streams in the considered solutions have dimensionless densities, bulk velocities and temperatures,  $n_1 = 1.609$ ,  $u_1 = (1.228; 0; 0)$ ,  $T_1 = 0.043$  and  $n_2 = 6.011$ ,  $u_2 = (0.329; 0; 0)$ ,  $T_2 = 0.603$ . The reference number density is  $N_{\text{ref}} = 10E+20$  and the reference temperature is  $T_{\text{ref}} = 7000$  K. These values of macroparameters correspond to downstream and upstream conditions of a normal shock wave with Mach number 6.5.

In Figure 3, solutions obtained using the BGK model with the improved velocity-dependent collision frequency, the BGK model with original-velocity dependent collision frequency and the classical BGK, ES-BGK and the Shakhov models are compared. The difference between the original and the improved velocity dependent collision frequencies is due to the way the relaxation rates for moments are enforced. In the original model, the number of enforced relaxation rates is equal to the number of the basis functions in the representation of the velocity dependent collision frequency. In particular, to enforce relaxation rates of high order moments, higher order polynomial basis functions are used. The use of high order polynomials results in strong perturbations of moments that are not enforced. An example of such perturbation can be seen in Figure 3(h). In this figure, relaxation of moments with kernels  $(u_i - v_i)^6$ ,  $i=1,2$ , are shown. Here  $v_i$ ,  $i=1,2,3$  are components of gas bulk velocity. These moments were not enforced in the simulations and appear to be strongly perturbed in the original model when high order moments are enforced. The improved model allows the number of enforced moments to be larger than the number of basis functions. In the new model, the coefficients of the collision frequency are determined by solving a linear least squares problem using singular value decomposition and regularization. In Figure 3(g), relaxation of moments  $(u_i - v_i)^6$ ,  $i=1,2$ , is shown in solutions computed by the improved model. The case marked by  $m=5$  corresponds to solutions in which moments with kernels  $(u_i - v_i)^m$ ,  $i=1,2$ ,  $m=3,4,5$  are enforced while only polynomials up to second degree were used in the representation of the collision frequency. It can be seen that the new model results in much smaller perturbations of moments that are not enforced as compared to the original model. In Figure 3(d—f) relaxation of the moments  $(u_i - v_i)^4$ ,  $i=1,2$ , is presented for solutions computed by the new model (d), the original model (e), and the classical models (f). In the original model only moments  $(u_i - v_i)^m$ ,  $i=1$ ,  $m=2,3,4,5$  are enforced and high order polynomials are used in the representation of the collision frequency to match the number of enforced moments. The results suggest that the new model approximates relaxation of high order moments comparable to the original model and better than the classical models. Nevertheless, as the number of enforced moments increases in the new model and the number of the basis

**DISTRIBUTION A.** Approved for public release: distribution unlimited.

functions is kept the same, it becomes difficult to achieve accurate rates for the moments because the residuals in the linear least squares solutions become large. This can be observed in Figure 3(a) where relaxation of the directional temperatures is presented. When only  $m=2$  moments are enforced, the use of new velocity-dependent collision frequency results in a reasonable approximation of the full Boltzmann equation. However, as the number of the enforced moments increases, the reconstruction of the second moment becomes worse.

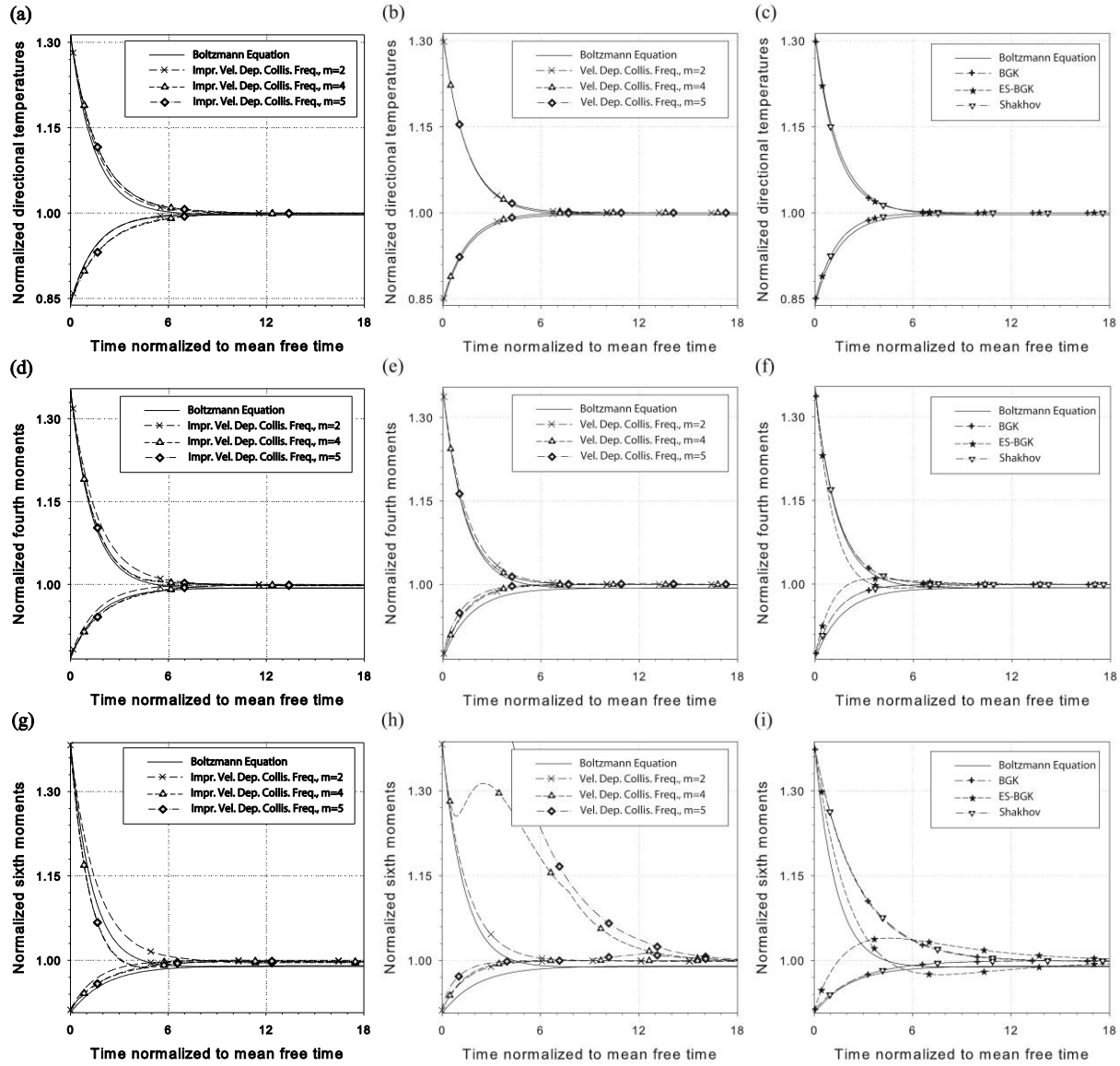


Figure 3. Relaxation of moments with kernels  $g_{i,m}=(u_i-v_i)^m$ ,  $i = 1; 2$ ,  $m = 2; 3; 4$  in a mix of Maxwellian streams corresponding to a shock wave with Mach number 6.5.

Overall, it was concluded that the new model is more stable and allows the approximation of the relaxation of the high order moments with a small number of the basis functions in the representation of the collision frequency. This is an advantage in 1D and 2D simulations as compared to the old model. Indeed, the solutions using new model would remained stable, while

DISTRIBUTION A. Approved for public release: distribution unlimited.

the solution using the old model crash for the same parameters of spatial and temporal discretizations. Stability of the old model can be restored, however, by increasing resolution in physical space and in time.

#### **2.4.2 Efficiency of the Evaluation of Boltzmann Collision Integral using Korobov Nodes**

The PI and the Graduate Assistant evaluated the accuracy and efficiency of the module that computes the Boltzmann collision integral using the Korobov nodes. It was observed that truncation errors of the Korobov integration decrease faster than the square root of the number of points for smooth solutions. It was also observed, however, that accuracy of the schemes for evaluation of the collision integral become acceptable (less than 1%) only for large numbers of Korobov nodes. Therefore, it was concluded that a number of nodes comparable but smaller than the number of nodes in full Gauss integration of the collision integral is required to achieve less than 1%  $l^2$ -error in the collision integral. As a result, while the method works correctly, it fails to provide significant acceleration as compared to the full deterministic integration. The PIs believe, however, that additional techniques can be devised that would allow the use of the method in the future. One technique that can be tried is the enforcement of conservation laws in the computed collision integral. The PI will study this approach in the future.

#### **2.4.3 Simulation of One Dimensional Supersonic Flow: the Normal Shock Wave**

The PIs applied the DGVlib library to the simulation of the problem of a normal shock wave. DGVlib was merged with a one-dimensional high-order Runge-Kutta discontinuous Galerkin (RKDG) solver available to the PI. The validity and accuracy of the library was tested by comparing to DSMC SMILE solutions and experimental results. Simulations were performed for normal shock waves with Mach numbers 1.55, 3.00, 3.8, 6.5, and 9.0. The results for shock waves 1.55 and 3.8 are presented in Figure 4 and Figure 5.

The parameters of the downstream and upstream boundary conditions are  $d_1=1.0676E-4 \text{ kg/m}^3$ ,  $v_1=500.018 \text{ m/s}$ ,  $T_1=300 \text{ K}$  and  $d_2=1.8990E-4 \text{ kg/m}^3$ ,  $v_2=281.098$ , in the case of the Mach 1.55 wave, and  $d_1=1.0676E-4 \text{ kg/m}^3$ ,  $v_1=1225.851 \text{ m/s}$ ,  $T_1=300 \text{ K}$  and  $d_2=3.35386E-4 \text{ kg/m}^3$ ,  $v_2=379.1322$ , in the case of the Mach 3.8 wave. The gas is argon with a specific heat ratio of 5/3. Solutions were computed using four different models. In the first model, the ES-BGK collision operator is used with the viscosity law of argon (power law exponent of .81). This solution is marked "ES-BGK Argon" in Figure 4(a, b). In the second model, the VD-BGK collision operator is used with the relaxation rate of the directional temperature in the x-direction enforced. The relaxation rates are computed from the Boltzmann collision operator with the interval of 20 mean free times using a hard spheres collision model. The diameter of the hard spheres is determined from the variable soft spheres model (VSS) so as to match the viscosity of the hard spheres gas to that of viscosity of argon. These solutions are marked "VD-BGK Argon" in Figure 4(a, b). In the third model, the ES-BGK collision operator is used with constants corresponding to the viscosity of the hard spheres gas with the diameter of hard spheres set to  $3.76E-10 \text{ m}$ . These solutions are marked "ES-BGK" in Figure 5(a)—(d). In the fourth model, the VD-BGK collision operator is used in which the relaxation rate of the directional temperature in the x direction is enforced. The relaxation rates are determined by evaluating the Boltzmann collision integral with the interval of 20 mean free times using the hard spheres model with the diameter of the hard spheres set to  $3.76E-10 \text{ m}$ . These solutions are marked "VD-BGK" in Figure

5(a)--(d). In Figure 64, density profiles of the computed solutions are compared to the experimental results of Alsmeyer [7]. In Figure 5, solutions are compared to the solution by DSMC solver SMILE.

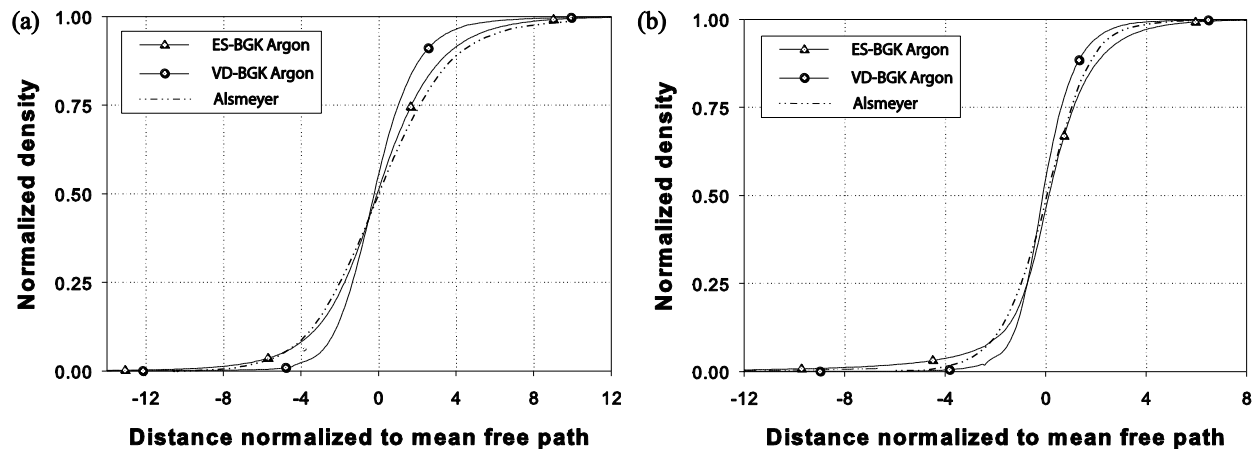


Figure 4. Plots of density and temperature profiles in solutions to the normal shock wave problem. Plot (a) corresponds to Mach number 1.55 and plot (b) to Mach number 3.8 shock waves.

In the case of the Mach 1.55 wave, the ES-BGK Argon solution is the closest to the experimental results. In the case of the Mach 3.8 wave, the VD-BGK Argon is somewhat closer to the experimental results than the ES-BGK Argon solution. However, neither ES-BGK nor VD-BGK model achieved a good accuracy. One reason why the VD-BGK model failed to approximate experimental results may be that the hard spheres collision model used to determine the enforced relaxation rates may not be the appropriate model to use for simulation of Mach 3.8 shock wave in argon. Nevertheless, results presented in Figure 4 illustrate well the fact that the DGVlib library enables the user to consider a whole range of collision models. Researchers will be able to select the model that fits the best in any particular case.

In Figure 5 solutions to Mach 3.8 shock wave obtained by ES-BGK model and BGK model with velocity-dependent collision frequency (VD-BGK) are compared to the solution obtained by DSMC solver SMILE. The density profile of the shock wave is presented in Figure 5(a). It can be seen that the VD-BGK solution predicts density profile before the shock better than the ES-BGK solution. However both VD-BGK and ES-BGK miss the DSMC solution after the shock. The velocity profile of the shock wave is shown in Figure 5(b). It can be seen that VD-BGK solution is significantly more accurate before the shock. After the shock the ES-BGK and VD-BGK solutions appear to be the same. In Figure 5(c) the temperature profile of the shock are presented and in Figure 5(d) the directional temperature  $T_x$  is shown. Again, it can be observed that VD-BGK solutions are significantly more accurate in front of the shock wave and appear about the same after the shock wave. Overall, it can be concluded that the VD-BGK model yielded improved physical accuracy of the model kinetic solutions as compared to ES-BGK model.

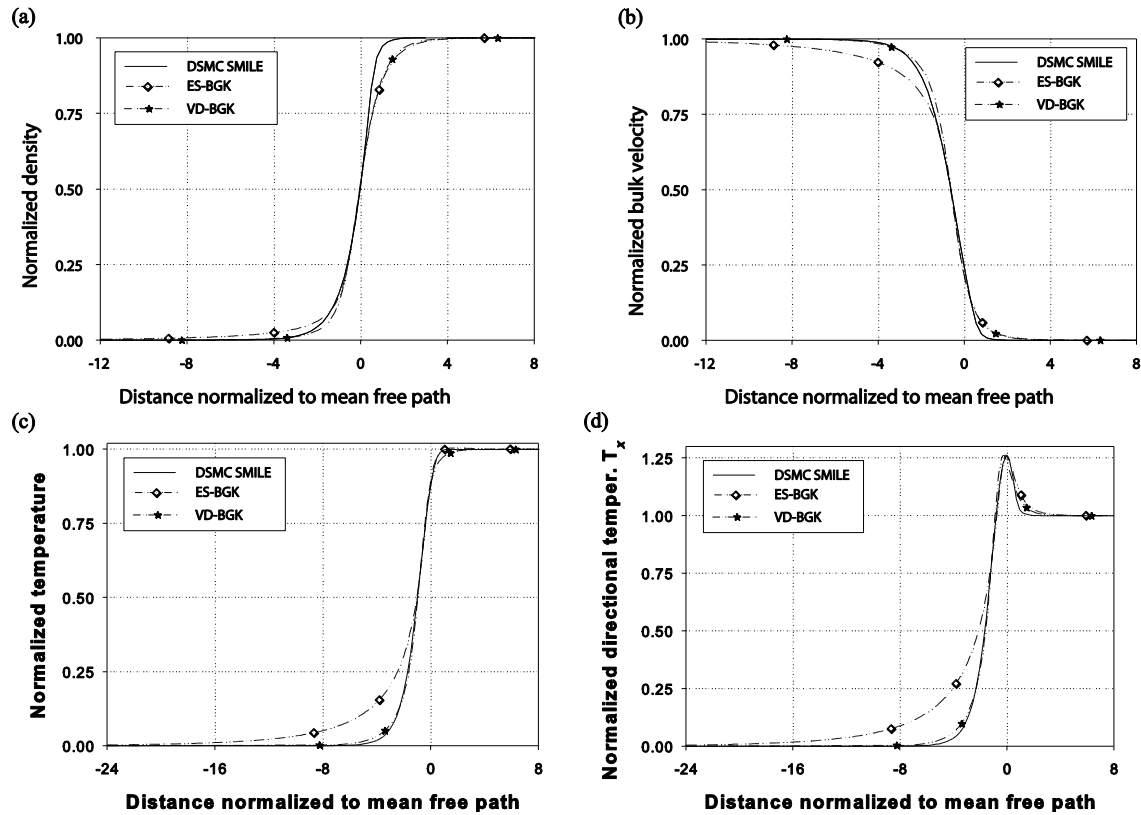


Figure 5. Solutions to normal shock wave with Mach 3.8 number.

#### 2.4.4 Simulation of Two-Dimensional Supersonic Flow around a Cylinder

The main objective of this task was to implement the program module for the solution of the right-hand side of the Boltzmann and model kinetic equations developed at CSUN into a kinetic solver SMOKE of Gimel Inc, and test the validity and accuracy of the module through comparison with benchmark solutions obtained by the DSMC solver SMILE. SMOKE [8] is a multi-dimensional finite volume solver to deterministically solve the BGK and ES-BGK model kinetic equations on parallel computers; it is based on conservative numerical schemes developed by L. Mieussens [9]. The kinetic and deterministic nature of SMOKE makes it an ideal testing ground for the developed program module. SMILE [10] is 2D/3D parallel code that uses the DSMC approach for the statistical solution of the full Boltzmann equation; it has been extensively validated for various problems through comparison with experimental data and other numerical solutions.

##### 2.4.4.1 Flow Conditions

The problem under consideration is supersonic flow over a two-dimensional cylinder. The free stream gas is nitrogen, mass density is  $1e-6$  kg/m<sup>3</sup>, temperature 250 K, and velocity 1,000 m/s. This corresponds to a  $\sim M=3$ ,  $Kn=0.1$  flow based on a 0.5 m cylinder diameter. Exponential viscosity - temperature dependence is used, with the exponent values of 0.5 (hard sphere model) and 0.75 used in the computations. The fully diffuse reflection on cylinder wall is used, with the wall temperature set first to 300 K and then to 500 K.

**DISTRIBUTION A.** Approved for public release: distribution unlimited.

### 2.4.4.2 Grid Convergence Study

Prior to the validation study and accuracy analysis, the spatial and velocity grid resolutions necessary for obtaining grid independent results were determined. The original SMOKE was used for this purpose. The number of spatial cells varied from 5,000 to over 25,000, and the number of velocity bins in each of the three directions varied from 20 to 60. An example of the convergence results is shown in Figure 6, where the gas macroparameters obtained for two different velocity grid resolutions are presented.

The example shows that even a 20x20x20 velocity grid resolution provides high accuracy in front of the cylinder, although there is some small difference in the wake flow where there are clearly more than 20 velocity points needed. The results showed that a velocity grid of 40x40x40, along with 5,000 spatial cells, provide adequate resolution as further refinement does not change the macroparameters.

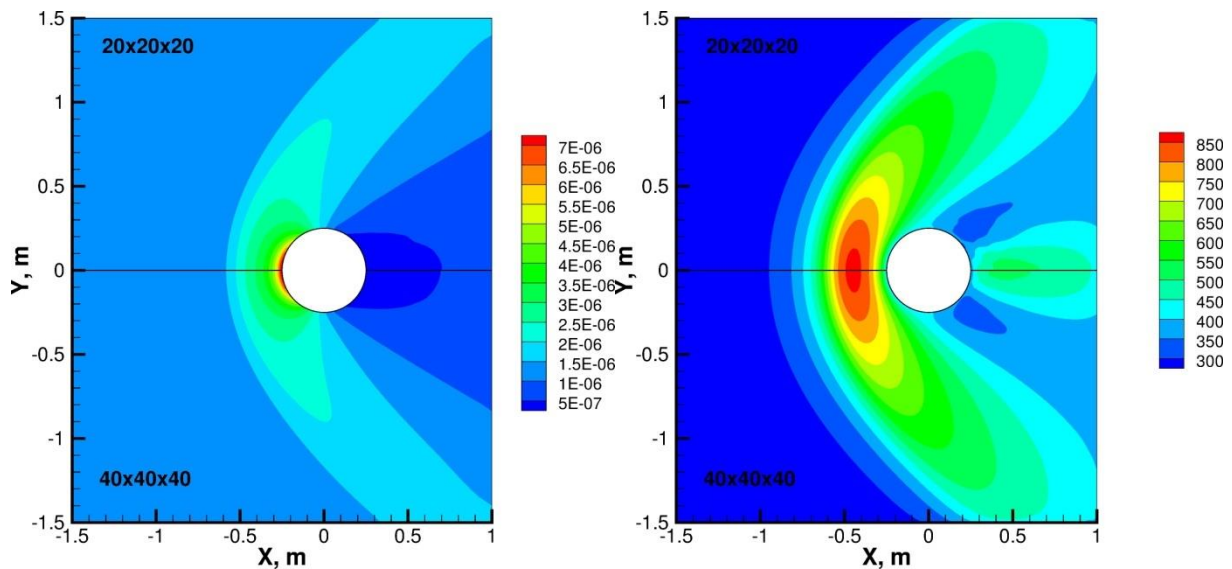


Figure 6. Density (left) and temperature (right) fields around a cylinder obtained for two different velocity grids (20x20x20, top, and 40x40x40, bottom, for X-Y-Z directions).  $T_{\text{wall}}=300$  K.

### 2.4.4.3 Adding ES-BGK Capability

The incorporation of the developed collision module into SMOKE allowed a direct comparison of the original and extended SMOKE (called SMOKE-DGV hereafter) in terms of the solution of the ES-BGK equation. Comparison of the two codes, SMOKE and SMOKE-DGV, is presented in Figure 7. One can see that there is quite reasonable agreement between the implementations, even though different methods of the solution of the ES-BGK equation are used. Good agreement between the codes provides verification of the implementation of the DGV extension.

As expected, the solution of the ES-BGK equation is noticeably different from the Boltzmann equation; consistent with similar comparisons published in the literature [11], the ES-BGK solution is characterized by a somewhat wider shock front. The difference in the wake region is less significant than that in the shock since the non-equilibrium is less pronounced in that region.

**DISTRIBUTION A.** Approved for public release: distribution unlimited.

Note that an ES-BGK solution is expected to be more accurate for Maxwellian molecules, and less accurate for hard spheres. This is illustrated in Figure 8, where the temperature fields obtained by SMILE and SMOKE-DGV are shown. It can be seen that, although there is good agreement in the wake region, the bow shock is much thicker in the ES-BGK solution.

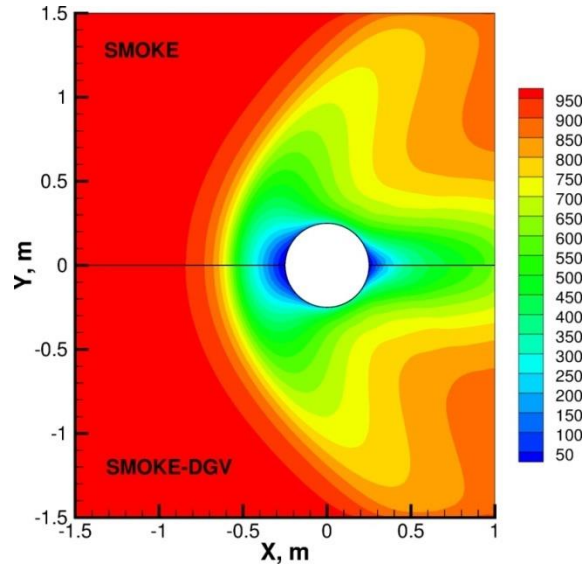


Figure 7. Velocity in X direction obtained by the solution of the ES-BGK equation with the original and extended SMOKE.

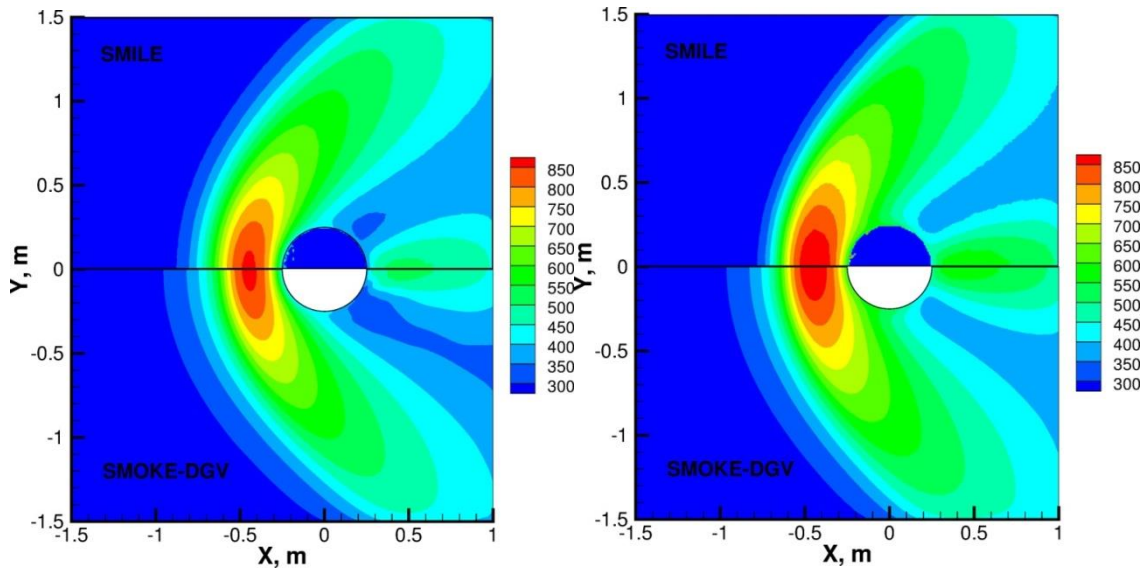


Figure 8. Comparison of the Boltzmann and ES-BGK solutions for Maxwellian molecules (left) and hard sphere molecules (right),  $T_{\text{wall}}=500$  K.

#### 2.4.4.4 BGK with Velocity-Dependent Collision Frequency: Correction through Boltzmann Equation

Let us now examine the effect of using a velocity-dependent collision frequency for the ES-BGK equation, obtained through the evaluation of the full Boltzmann collision integral. The gas properties obtained for the hard sphere model are presented in Figure 9. Here, the bottom halves show the results computed with extended SMOKE ES-BGK models (SMOKE-DGV) and the model with velocity-dependent collision frequency (SMOKE-vDGV). It can be seen that the correction of the collision frequency allows for much closer agreement with the solution of the Boltzmann equation. Note that the correction was conducted about every 500-th time step, and the total computational time increased by approximately 50%. Still, further refinement through the increase in the resolution of the velocity grid during the evaluation of the Boltzmann collision integral (currently at 15x15x15) requires significantly larger computer resources, and thus efficient parallelization.

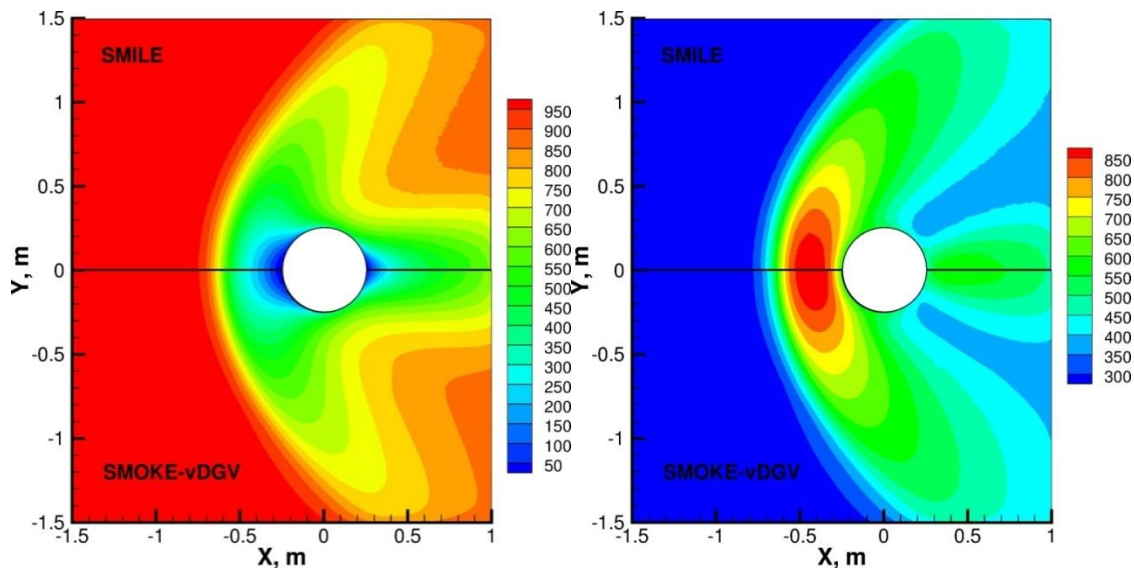


Figure 9. Velocity field (left) and temperature (right) obtained by the solution of the Boltzmann equation (top halves) and velocity-dependent ES-BGK (bottom halves).

Also note that a non-equilibrium dependent switch has been used between the regular and velocity-dependent modes of the ES-BGK equation. In regions where non-equilibrium is significant, the velocity-dependent mode is used, while in the rest of the domain, the conventional ES-BGK equation is solved. The degree of non-equilibrium is evaluated by the  $\Delta f = |f - f_{eq}|/f$  metric, where  $f$  and  $f_{eq}$  are the local computed and corresponding equilibrium distribution functions. The values of this metric are given in Figure 10. The velocity-dependent collision frequency was used in regions where  $\Delta f > 0.05$ .

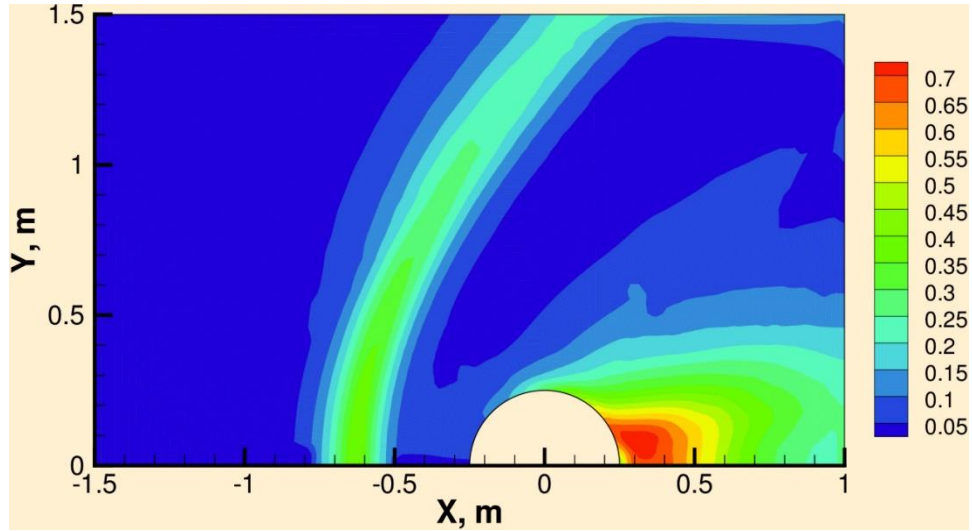


Figure 10. Non-equilibrium metric used for switching between conventional and velocity-dependent frequency ES-BGK equations.

### 3. SUMMARY

New modules for evaluating the kinetic collision operator using BGK model with velocity-dependent collision frequency (VD-BGK) and for evaluating the Boltzmann collision integral using quasi-stochastic integration have been implemented. Benchmark solutions have been computed to test the VD-BGK model. Solutions were compared to DSMC solutions and experimental results.

In zero, one- and two-dimensional simulations it was observed that the Boltzmann equation based correction to the collision frequency improves agreement with the solution of the Boltzmann equation as compared to the classical ES-BGK model equations. One difficulty that persists is the fact that the VD-BGK model makes the kinetic equation considerably stiffer when high order moments are enforced. The new least-squares approach helps to reduce the stiffness significantly, however, different forms of velocity-dependent collision frequency may need to be explored to remedy the excess stiffness entirely. The need to evaluate the Boltzmann collision operator to estimate relaxation rates of the moments in the VD-BGK model is limiting efficiency of the model, especially for two dimensional problems. The introduction of coarser secondary grid in DGVlib for such estimates did improve the efficiency. However, shock waves with high Mach numbers still require large secondary grids. A possible remedy to that may be a direct computation of the moments of the collision operator bypassing the evaluation of the collision operator itself. These evaluations are orders of magnitude faster than evaluations of the full collision integral, but require significantly more memory for storing pre-computed moment kernels. Formulating and implementing this approach will be PIs future work.

Korobov integration of the collision integral proved to be more evasive than originally thought. It was observed that Korobov quadratures do converge to the desired integral. However, practically acceptable levels of errors are achieved only for numbers of integration points

**DISTRIBUTION A.** Approved for public release: distribution unlimited.

comparable to those in full deterministic evaluation of the collision integral. The PIs hope, however, that additional remedies can be introduced to the method, e.g., enforcement of conservation laws in the computed collision integral. These remedies would allow use of smaller number of quadrature points. The proposed future modification of the methods could be implemented in DGVlib with a minor programming effort. Therefore, DGVlib represents a flexible software tool that can be easily modified to improve the models.

#### 4. REFERENCES

- [1] A. Alekseenko and E. Josyula. Deterministic solution of the spatially homogeneous Boltzmann equation using discontinuous Galerkin discretizations in the velocity space. *Journal of Computational Physics*, 272(0):170-188, 2014.
- [2] A. Alekseenko and C. Euler. A Bhatnagar-Gross-Krook kinetic model with velocity-dependent collision frequency and corrected relaxation of moments. *Continuum Mechanics and Thermodynamics*, 2015, DOI 10.1007/s00161-014-0407-0
- [3] F. Golse. The Boltzmann equation and its hydrodynamic limits. *Volume 2 of Handbook of Differential Equations: Evolutionary Equations*, pages 159-301. North-Holland, 2006
- [4] F. G., Tcheremissine, Solution to the Boltzmann kinetic equation for high-speed flows. *Computational Mathematics and Mathematical Physics*, 46(2):315–329, 2006.
- [5] N.M. Korobov, *Exponential sums and their applications*. Mathematics and its applications. Soviet series; V. 80. Kluwer Academic Publishers, 1992
- [6] Interim Technical Report for the Project PP-SAS-KY06-001-P3, November 2014
- [7] H. Alsmeyer, Density profiles in argon and nitrogen shock waves measured by the absorption of an electron beam. *Journal of Fluid Mechanics* 1976, **74** (3) pp. 497—513.
- [8] N. Gimelshein, S. Gimelshein, N. Selden, A. Ketsdever, Modeling of low-speed rarefied gas flows using a combined ES-BGK/DSMC approach, *Vacuum*, 2010, **85** (2) pp. 115-119.
- [9] L. Mieussens, "Discrete-Velocity Models and Numerical Schemes for the Boltzmann-BGK Equation in Plane and Axisymmetric Geometries," *J. Comp. Physics*, 2000, **162** pp. 429-466.
- [10] M.S. Ivanov, G.N. Markelov, S.F. Gimelshein, "Statistical simulation of reactive rarefied flows: numerical approach and applications," *AIAA Paper 98-2669*, June 1998.
- [11] D. C. Wadsworth, N.E. Gimelshein, S. F. Gimelshein, I.J. Wysong, "Assessment of Translational Anisotropy in Rarefied Flows Using Kinetic Approaches," *Proc. XXVI Int. Symp. on Rarefied Gas Dynamics*, Kyoto, Japan, July 2008.